

Distribution and Role of Trace Transition Metals in *Glycera* Worm Jaws Studied with Synchrotron Microbeam Techniques

Helga C. Lichtenegger,^{*,†} Henrik Birkedal,[‡] Diego M. Casa,[§] Julie O. Cross,[§]
Steve M. Heald,^{||} J. Herbert Waite,^{*,⊥} and Galen D. Stucky^{*,#}

Institute of Materials Science and Technology (E308), Vienna University of Technology, Favoritenstr. 9-11, A-1040 Wien, Austria, Department of Chemistry and Interdisciplinary Nanoscience Center (iNANO), University of Aarhus, Aarhus, Denmark, Advanced Photon Source, Argonne National Laboratory, Argonne, Illinois, Pacific Northwest National Laboratory, Richland, Washington, Department of Molecular, Cellular and Developmental Biology, University of California, Santa Barbara, Santa Barbara, California 93106, and Department of Chemistry, University of California, Santa Barbara, Santa Barbara, California 93106

Received January 31, 2005. Revised Manuscript Received March 14, 2005

A combination of position-resolved synchrotron microbeam techniques was used to explore the distribution and role of trace transition metals in the jaws of *Glycera dibranchiata*. The mandibles of this marine sediment worm have recently been found to be reinforced by the copper-based biomineral atacamite [Cu₂(OH)₃Cl]. Here we show that the system is more complex, containing zinc and iron and unmineralized copper compounds as well. X-ray absorption spectroscopy studies showed that a fraction of copper is present in oxidation state, Cu(I), in contrast to the mineral that exclusively contains Cu(II). X-ray fluorescence imaging revealed traces of copper also in the jaw base devoid of mineral. Traces of iron were found as well, but occurred spatially correlated with the copper mineral, suggesting a substitution of copper atoms by iron in the atacamite mineral. Zinc was evenly dispersed throughout the jaw matrix, quite in analogy to zinc in *Nereis* jaw, a related worm species, where nonmineralized zinc serves to cross-link and harden the proteinaceous matrix.

Introduction

Marine invertebrates often contain peculiar types of hard tissue in contrast to vertebrate teeth and bone that are mainly hardened by calcium-based biominerals. The teeth of chitons for example are hardened by magnetite¹ and certain polychaete worms rely on copper or zinc.^{2–6} A rare copper mineral (atacamite) was recently discovered in the jaws of the marine polychaete *Glycera dibranchiata*,⁵ representing a so far unique case of copper biomineralization.⁷ *Glycera* jaws are syringelike and used by the worm to inject a neurotoxic venom into its prey.^{8,9} Atacamite [Cu₂(OH)₃Cl]

is deposited in an organic matrix and forms ~80 nm thick polycrystalline fibers that run parallel to the outline of the jaw tip and enhance the jaw hardness. Compared to other mineralized tissues, the mineral content of *Glycera* jaw is very low, the major part of the jaw material (up to 90%) being organic with a protein content of about 60% (mostly glycine and histidine).⁵ Notably, the amino acid composition resembles that found in the jaws of *Nereis*, a related worm species that uses zinc rather than copper to harden its mandibles, however, in the nonmineralized form.⁶ In a previous study, it was found that *Glycera* jaws contain more copper than can be attributed to the atacamite mineral (calculated from the Cu/Cl ratio in the jaw as compared to that in the mineral),¹⁰ but its nature was not further explored. Here we use a combination of several state-of-the-art synchrotron microfocus techniques such as X-ray fluorescence imaging (XFI), X-ray absorption spectroscopy (XAS), anomalous small-angle X-ray scattering (aSAXS), and microdiffraction (micro-XRD) to study the distribution and role of unmineralized copper and other inorganic trace components such as zinc and iron in the *Glycera* jaw.

Experimental Section

Sample Preparation. *Glycera* worm jaws were obtained from the Marine Biological Laboratory in Woods Hole, MA, and deep frozen upon arrival. Jaws were dissected from the animal, washed in artificial seawater and deionized water, and dried. For all

* Authors to whom correspondence should be addressed. (H.C.L.) Fax: (+43)-1-58801-30895. E-mail: helga.lichtenegger@tuwien.ac.at. (J.H.W.) Fax: +1-805-893-7998. E-mail: waite@lifesci.ucsb.edu. (G.D.S.) Fax: +1-805-893-4120. E-mail: stucky@chem.ucsb.edu.

[†] Vienna University of Technology.

[‡] University of Aarhus.

[§] Argonne National Laboratory.

^{||} Pacific Northwest National Laboratory.

[⊥] Department of Molecular, Cellular, and Developmental Biology, University of California, Santa Barbara.

[#] Department of Chemistry, University of California, Santa Barbara.

- (1) Lowenstam, H. A. *Science* **1967**, *156*, 1373.
- (2) Bryan, G. W.; Gibbs, P. E. *J. Mar. Biol. Assoc. U.K.* **1979**, *59*, 969.
- (3) Bryan, G. W.; Gibbs, P. E. *J. Mar. Biol. Assoc. U.K.* **1980**, *60*, 641.
- (4) Gibbs, P. E.; Bryan, G. W. *J. Mar. Biol. Assoc. U.K.* **1980**, *60*, 205.
- (5) Lichtenegger, H. C.; Schöberl, T.; Bartl, M. H.; Waite, J. H.; Stucky, G. D. *Science* **2002**, *298*, 389.
- (6) Lichtenegger, H. C.; Schöberl, T.; Ruokolainen, J. T.; Cross, J. O.; Heald, S. M.; Birkedal, H.; Waite, J. H.; Stucky, G. D. *Proc. Natl. Acad. Sci. U.S.A.* **2003**, *100*, 9144.
- (7) Weiner, S.; Addadi, L. *Science* **2002**, *298*, 375.
- (8) Michel, C. *Cah. Biol. Mar.* **1970**, *11*, 209.
- (9) Meunier, F. A.; Feng, Z. P.; Molgo, J.; Zamponi, G. W.; Schiavo, G. *EMBO J.* **2002**, *21*, 6733.

- (10) Lichtenegger, H. C.; Schöberl, T.; Bartl, M. H.; Waite, H.; Stucky, G. D. *Science* **2003**, *301*.

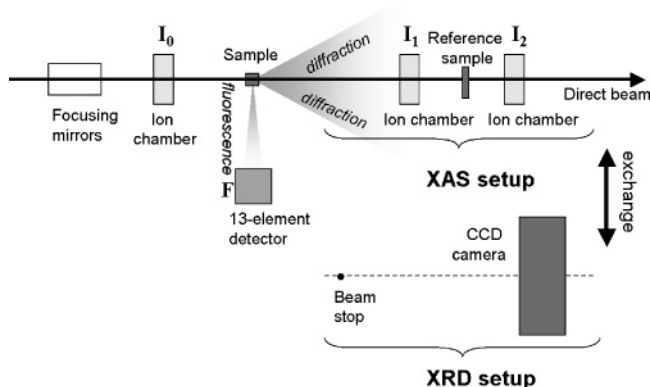


Figure 1. Experimental setup for combined XFI, XAS, and micro-XRD measurements at beamline 20 ID, PNC-CAT, APS (Argonne National Laboratory). The configuration allowed a combination of micro XAS, XFI, and micro-XRD measurements with a position resolution of 5 μm .

experiments, excepting microdiffraction, intact jaws were used without further treatment, simply mounted on thin glass fibers with a small drop of superglue. For microdiffraction, jaws were embedded in epoxy resin and 2 μm thick cross sections were cut from the jaw tip with an ultramicrotome equipped with a glass knife. The sections were picked up from the knife and directly transferred to adhesive Kapton tape.

Measurements. Synchrotron microfocus experiments on *Glycera* jaws were carried out at the Advanced Photon Source (APS), Argonne National Laboratory, U.S.A. Techniques included XFI, XAS, micro-XRD, and aSAXS. Experiments were done with a position resolution (beam size) ranging from 0.1 mm (Complex Materials Consortium, CMC-CAT beamlines) down to 5 μm (Pacific Northwestern Consortium, PNC-CAT beamlines). Such small beam sizes allow detailed and nondestructive imaging with micrometer resolution.^{11,12}

Fluorescence Imaging, XAS, and Micro-XRD. Experiments were done at PNC-CAT, beamlines 20 ID and 20 BM. The experimental layout at beamline 20 ID was specially configured to combine all of the above techniques without having to touch the sample. This is crucial for scans with micrometer position resolution in order to be able to reproducibly correlate results from different measurements. The setup scheme is shown in Figure 1: the X-ray beam first passes mirrors where its diameter gets reduced to a size of 5 μm at the sample position. An ion chamber records the intensity of the beam before it enters the sample (I_0). A second ion chamber positioned behind the sample measures the intensity transmitted by the sample (I_1). The fluorescence signal from the sample, F , is recorded by a 13-element detector positioned at right angles to the sample. Part of this setup (marked "XAS setup" in Figure 1 and comprising the two ion chambers positioned behind the sample) could be moved out of the beam and replaced by a beamstop and a charge-coupled device (CCD) camera (Bruker AXS, Madison) in order to record X-ray diffraction (XRD) from the sample ("XRD" setup in Figure 1).

For XFI, the energy of the incident beam was set to 11 keV, which is well above the absorption edges of Cu, Zn, and Fe, to excite fluorescence from these elements. The sample was scanned through the beam in 5- μm steps. The software EPICS was used to control the step motors, record the fluorescence signal F at every point, normalize it to the primary intensity (F/I_0), and combine the values of each point to yield 2-D maps for each element. The

element maps were then used to select different points in the Cu containing *Glycera* jaw tip for subsequent XAS.

For XAS, the energy of the incident beam was scanned across the absorption edge of copper, and I_0 , I_1 , and F were recorded as a function of energy E . The absorption coefficient μ of the sample was calculated from $\mu(E) = \ln(I_0/I_1)$ (absorption measurement) and $\mu(E) = F/I_0$ (fluorescence measurement), respectively. A Cu foil was inserted as a reference sample; its transmission I_1/I_2 was recorded during each measurement, and the reference curves were used for energy calibration. The XAS of pure atacamite mineral powder was measured at beamline 20 BM. The beam diameter at 20 BM was larger (1 mm) and therefore more suitable for the measurement of powder standards due to averaging over a greater number of crystallites. The powder was packed into flat sachets of adhesive Kapton tape, mounted on a copper stage, and inserted into a cryostat and cooled to 4 K in order to enhance the XAS signal.

X-ray absorption near edge structure (XANES) data were background corrected and normalized. Extended X-ray absorption fine structure (EXAFS) data were background corrected, normalized, and converted to $\chi(k)$ with $k = 2\pi/\lambda$ being the wave vector, where λ is the wavelength of the incident beam. EXAFS spectra were fitted with a theoretical atacamite standard calculated using the software FEFF8.^{13,14}

XFI and micro-XRD mapping were combined on cross sections of *Glycera* jaw tip in order to investigate the spatial correlation of elevated Cu and Cl levels and the occurrence of diffracting atacamite mineral. First, Cu and Cl fluorescence images were recorded in a 2-D scan with a step size of 5 μm . I_0 and I_1 were monitored and used to calculate the transmission of the sample I_1/I_0 . Subsequently, the "XAS setup" (Figure 1) was changed to "XRD setup". The scan was repeated, and diffraction images were taken at each point. The XRD patterns were normalized with respect to I_0 and corrected for transmission. The intensity of the (011) reflection (strongest reflection of atacamite¹⁵) was integrated over the azimuth to reduce effects due to preferred crystallographic orientation (texture) as far as possible, the intensity values were associated with a gray level, and the result arranged into a 2-D intensity map of the sample.

aSAXS. aSAXS experiments were carried out at beamline 9 ID, CMC-CAT. Sample, beamstop, and CCD camera were all positioned in one line, with the detector at a distance of 5.25 m from the sample. The diameter of the X-ray beam was 0.1 mm. Scattering patterns of the atacamite-containing *Glycera* jaw tip were recorded at variable photon energies in the vicinity of the Cu (8.79 keV) and Zn (9.66 keV) K-absorption edges, respectively. The flight path of the scattered photons was evacuated to reduce air scattering. The intensity of the incident beam I_0 was monitored continuously using an ion chamber. The absorption of the sample at various energies was measured with a PIN diode prior to each SAXS scan. The 2-D SAXS patterns read from the CCD camera were normalized with respect to I_0 , background corrected, and corrected for absorption. Next, the 2-D scattering images were integrated over the azimuth and the intensity plotted vs the scattering vector q to give scattering curves, where $q = 4\pi/\lambda(\sin \theta)$, with 2θ denoting the scattering angle and λ the wavelength.

Results and Discussion

Micro-XFI was used to probe the detailed distribution of transition metals in *Glycera* jaw; results are presented in

(11) Paris, O.; Zizak, I.; Lichtenegger, H.; Roschger, P.; Klaushofer, K.; Fratzi, P. *Cell. Mol. Biol.* **2000**, *46*, 993.
 (12) DiMasi, E.; Sarikaya, M. *J. Mater. Res.* **2004**, *19*, 1471.

(13) Ankudinov, A. L.; Ravel, B.; Rehr, J. J.; Conradson, S. D. *Phys. Rev. B* **1998**, *58*, 7565.
 (14) Ankudinov, A. L.; Bouldin, C. E.; Rehr, J. J.; Sims, J.; Hung, H. *Phys. Rev. B* **2002**, *65*, 104107/1.
 (15) Parise, J. B.; Hyde, B. G. *Acta Crystallogr., Sect. C* **1986**, *42*, 1277.

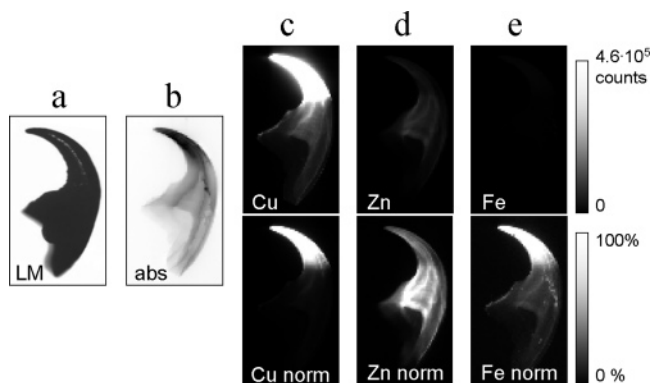


Figure 2. Element distribution in *Glycera* jaw determined by XFI. (a) LM image of a *Glycera* jaw. The syringe needlelike tip of the jaw is used by the worm to inject venom. (b) X-ray absorption image: dark regions correspond to greater absorption by the sample. The tip of the *Glycera* jaw is less X-ray transparent than the rest of the jaw. (c–e) Fluorescence maps of Cu, Zn, and Fe. The maps in the upper row were gray scaled according to the original counts measured by the fluorescence detector (normalized only to the primary beam intensity) and, therefore, give a crude estimate of the concentration of each element. For the maps in the bottom row (Cu norm, Zn norm, and Fe norm) the brightness was normalized to the maximum value of fluorescence counts in each image to better visualize the element distribution. The gray scale bar denotes the absolute number of counts in the upper row and percent of the maximum intensity in the bottom row, respectively.

Figure 2. A light microscope (LM) image of a *Glycera* jaw is displayed in Figure 2a; the jaw material is smooth and jet-black, and no differences between tip and base are visible to the naked eye. The X-ray absorption image in Figure 2b shows that the tip region of the jaw is less transparent for X-rays than the rest of the jaw (brighter gray denotes higher X-ray transmission). The XFI maps in parts c–e of Figure 2 illustrate the Cu, Zn, and Fe distribution in *Glycera* jaw. For the maps in the upper row, the brightness was set proportional to the measured fluorescence intensity, which gives a crude estimate of the actual element concentration. Large amounts of Cu are obviously present in the jaw tip that contains the copper-based atacamite biomineral.⁵ By normalization of the XFI images to their respective maximum intensity (parts c–e of Figure 2, bottom row), the distribution of the trace elements Zn and Fe becomes clearer: whereas Fe is largely restricted to the jaw tip, the Zn concentration is fairly constant throughout the whole jaw. The occurrence of Fe exclusively in the tip can be attributed to an iron contamination of the atacamite biomineral [Cu₂(OH)₃Cl]: the naturally occurring mineral hibbingite [Fe₂(OH)₃Cl] has the exact same crystal structure as atacamite.¹⁶ Fe atoms may simply substitute Cu in atacamite thus forming a solid solution.

Zinc, on the contrary, occurs completely uncorrelated with the Cu mineral and is evenly dispersed throughout the jaw matrix. Notably, Zn appears to be a common element in polychaetes: it was also found in the jaws of *Nereis limbata*, another polychaete worm, where it occurs in higher concentration than in *Glycera* jaw but also in the nonmineralized form.⁶ The amino acid compositions of *Glycera* and *Nereis* jaws show striking similarities, with Gly and His being the predominant components in the jaw matrix of both worm species.^{5,6} In *Nereis* jaw, Zn, Cl, and His levels are correlated

and X-ray absorption experiments have suggested that Zn ions may be coordinated by His and Cl,⁶ quite similar to the conformation found in the center of the Zn insulin hexamer.¹⁷ Given the His-rich composition of *Glycera* jaws,⁵ here the protein matrix may be involved in Zn binding. Since in contrast to *Nereis* jaw, Cl was not found in the matrix of the *Glycera* jaw,¹⁰ a zinc-insulin-type coordination can be excluded; as Cys was not detectable in the *Glycera* jaw, a zinc-finger motif can be excluded as well. Still, the variety of remaining possibilities of Zn–His coordination is considerable.¹⁸ Zn XAS would be a suitable method to obtain further information, but the XAS signal was too weak to yield useful information.

Zinc is not the only metal dispersed in the jaw matrix: traces of Cu are also found throughout the jaw in addition to the Cu-based mineral in the jaw tip (Figure 2b). Energy-dispersive X-ray analysis experiments on transmission electron microscopy (TEM) sections from the jaw tip have shown that also the matrix between adjacent atacamite-reinforced fibers contains some Cu.¹⁰ Other researchers have suggested that there may be more Cu compounds in the jaw, different from atacamite, and perhaps in even greater abundance.¹⁹

XAS is a very sensitive tool for the identification of chemical compounds and was used here to screen the jaw for any copper compounds different from atacamite. XAS experiments were done on *Glycera* jaw tips and pure atacamite mineral for comparison. Figure 3a compares Cu K-edge XANES signals from *Glycera* jaws and atacamite powder. The spectra strongly resemble each other, suggesting that most of the Cu in *Glycera* jaw is present as atacamite. The extra pre-edge peak in the jaw spectrum, however, is a clear indicator for the presence of Cu(I), whereas in atacamite all the copper is present as Cu(II). Parts b and c of Figure 3 compare the EXAFS curves obtained from *Glycera* jaw with a fit using a theoretical atacamite standard calculated with the software FEFF8.^{13,14} Whereas the major part of the spectrum is well modeled by the atacamite standard, there is a small mismatch around 2 Å in the *R* spectrum. This corresponds well with the finding that most of the Cu is mineral bound with a small amount of nonatacamite, Cu(I)-containing compounds. There are several possibilities for the function of excess Cu: first, Cu ions could be coordinated by His just as well as Zn; the high affinity of His to transition metals is well known.²⁰ Copper could also have a function different from mechanical stabilization; in fact, a great number of copper enzymes contain Cu(I).

Whereas the XAS experiment above shows that the major fraction of Cu resides in the same chemical environment as atacamite, it is not sensitive to crystallinity. Amorphous inorganic phases are not uncommon in biology and may occur in the place of or in addition to crystalline forms.^{21–24}

(17) Berman, H. M.; Westbrook, J.; Feng, Z.; Gilliland, G.; Bhat, T. N.; Weissig, H.; Shindyalov, I. N.; Bourne, P. E. *Nucleic Acids Res.* **2000**, *28*, 235.

(18) Vallee, B. L.; Auld, D. S. *Biochemistry* **1990**, *29*, 5647.

(19) Schofield, R. M. S.; Nesson, M. H. *Science* **2003**, *301*.

(20) Morgan, W. T. *Biochemistry* **1984**, *24*, 1496.

(21) Taylor, M. G.; Simkiss, K.; Greaves, G. N.; Okazaki, M.; Mann, S. *Proc. R. Soc. London, Ser. B* **1993**, *252*, 75.

(16) Sainieidukat, B.; Kucha, H.; Keppler, H. *Am. Miner.* **1994**, *79*, 555.

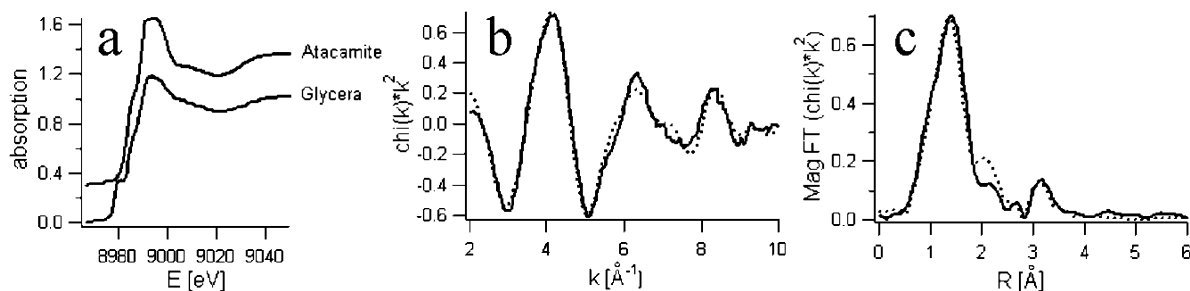


Figure 3. XAS of *Glycera* jaw. (a) XANES spectra of *Glycera* jaw and atacamite in comparison (the atacamite spectrum is shifted vertically for better visibility). The extra pre-edge peak in the *Glycera* spectrum is indicative of Cu(I). (b) Cu EXAFS spectra of *Glycera* jaw tip in k space. The solid line corresponds to data from *Glycera* jaw, the dashed line is a fit to the data with a theoretical atacamite standard calculated using the software FEFF8. (c) EXAFS signal from *Glycera* jaw in R space. There are small discrepancies between the *Glycera* data and the atacamite fit at around 2 Å.

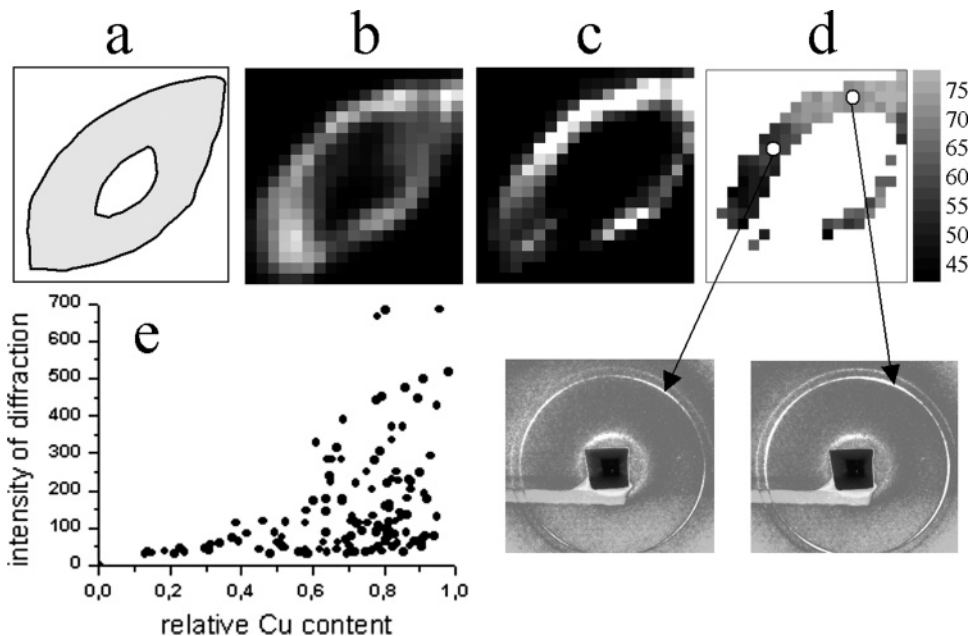


Figure 4. Combined XFI and micro-XRD mapping on a transverse cross section of *Glycera* jaw tip. (a) Sketch of the sample: gray regions denote sample material, the hole in the middle is a cross section through the venom canal. (b) Cu XFI map of the sample reveals that the Cu is mainly concentrated in the vicinity of the outer jaw surface. (c) Results from a diffraction scan: the intensity map was compiled from an array of diffraction patterns and the gray value in each pixel represents the intensity of the (011) reflection of atacamite (strongest reflection) integrated over the azimuth. (d) Variation of azimuthal distribution of the (011) intensity. The gray scale denotes the azimuthal orientation of the intensity maximum (in degrees). The XRD patterns below are typical examples. (e) Combination of the Cu XFI map in b and the diffraction map in c allowed a quantitative correlation of relative Cu content (calculated as the local fluorescence intensity divided by the maximum intensity in the XFI map) and the amount of diffracting atacamite mineral.

To get a rough estimate on the amount of crystalline and noncrystalline copper compounds in the jaw, we used a combination of XFI and micro-XRD mapping on a thin cross section of *Glycera* jaw tip (sketched in Figure 4a). The XFI map in Figure 4b shows the local Cu distribution. Subsequent to XFI, micro-XRD imaging was carried out on the same sample. The intensity of the (011) reflection was taken as an indicator of the amount of crystalline material, and the intensity values were compiled into a 2-D intensity map (Figure 4c). A quantitative plot of the (011) intensity vs the relative local copper content (fluorescence counts normalized by maximum counts of scan) reveals a positive correlation (Figure 4e), indicating that a higher Cu content is linked to a higher amount of diffracting mineral. Notably, however, there are some regions with high Cu content and apparently

low diffraction intensity. Since the fraction of Cu(I)-containing compounds detected by XAS is very minor and can hardly account for this effect, part of the mineral may indeed be nondiffracting; it should be noted, however, that the result is most likely influenced by preferred crystallographic orientation of atacamite crystallites (texture), leading to an orientation dependence of the observed intensity and possibly causing artifacts. In fact, the crystallographic orientation is not random, but the intensity of the (011) reflections varies over the azimuth (see example XRD patterns in Figure 4). In Figure 4d, the azimuthal orientation of the XRD pattern is compiled into an orientation map, revealing a systematic smooth change over the sample cross section (the gray values denote the orientation in degrees).

Given the detection of at least a small fraction of nonmineralized copper compounds, it becomes interesting to re-examine the localization of copper in the jaw. aSAXS is a useful tool to check by contrast variation whether copper is mainly restricted to the mineralized fibers or distributed otherwise. The fibrous structure of the jaw tip yields a typical,

(22) Beniash, E.; Aizenberg, J.; Addadi, L.; Weiner, S. *Proc. R. Soc. London, Ser. B* **1997**, *264*, 461.

(23) Aizenberg, J.; Weiner, S.; Addadi, L. *Connect. Tissue Res.* **2003**, *44*, 20.

(24) Olszta, M. J.; Odom, D. J.; Douglas, E. P.; Gower, L. B. *Connect. Tissue Res.* **2003**, *44*, 326.

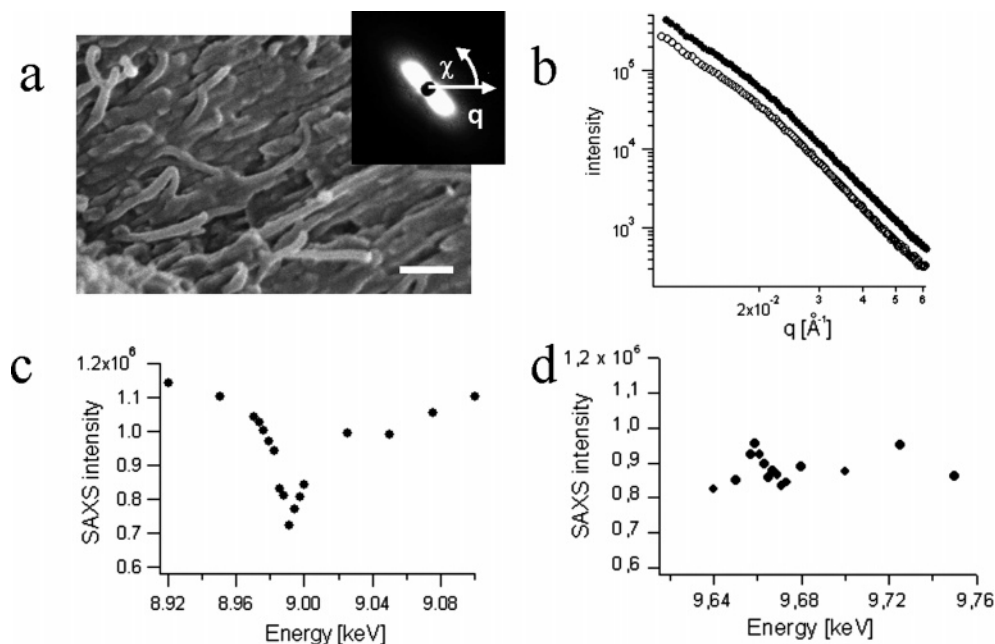


Figure 5. aSAXS of *Glycera* jaw. (a) SEM image of fibrous structure of *Glycera* jaw tip, scale bar = 0.5 μm . Inset: typical elongated SAXS pattern resulting from a fiber structure. (b) SAXS curves obtained by integrating 2-D patterns (as shown in a) over the azimuth χ and plotting the intensity vs the scattering vector q , where $q = 4\pi/\lambda \sin(\theta)$ with λ being the X-ray wavelength and θ half the scattering angle, 2θ . Curves displayed were recorded at X-ray energies below (full symbols) and close to the Cu K absorption edge (open symbols). Note the logarithmic scale. (c) Total SAXS intensity (area under the SAXS curves) as a function of incident energy. There is a pronounced minimum at the Cu K edge (8.98 keV). (d) The SAXS intensity as a function of energy in the vicinity of the Zn K edge (9.66 keV). The SAXS intensity is essentially constant.

elliptical SAXS pattern, with the short axis denoting the fiber direction (Figure 5a). The energy of the incident beam was scanned across the Cu K absorption edge (8.98 keV), and while the shape of the SAXS pattern did not change, changes in the scattered intensity were observed. Figure 5b shows scattering curves below (full circles) and at the Cu K edge (open circles), respectively (note the logarithmic scale). Figure 5c displays the total SAXS intensity (the area under each SAXS curve) vs energy, giving a smooth function that reaches its minimum about 8.98 keV. This result corresponds to what would be expected for a fibrous system where a considerable part of the scattering contrast is due to an element contrast between fiber and matrix,²⁵ thus suggesting that a major fraction of the Cu is located in the mineralized fibers. The aSAXS experiment was repeated at the Zn K edge (9.66 keV). Almost no variation of the SAXS intensity was observed (Figure 5d), which is consistent with a homogeneous Zn distribution. It should be noted, however, that the overall Zn concentration in *Glycera* jaws is very low, which may result in a Zn aSAXS signal too weak to be detected. Nevertheless, a restriction of Zn to the mineralized fibers seems highly unlikely given the occurrence of Zn in the jaw base as well as the mineralized tip.

In summary, we have found that *Glycera* worm jaws represent a biological system that combines an organic matrix with crystalline as well as noncrystalline forms of transition metals. The copper-based biomineral atacamite coexists with

traces of unmineralized copper, where a fraction is in oxidation state, Cu(I). Zn is dispersed throughout the jaw and most likely acts as a cross-linker of the protein matrix through His coordination. Iron is found in trace quantities and restricted to the mineral-rich tip region and we suggest that it can be attributed to Fe-substitution in atacamite. Multifunctionality and coexistence of crystalline and non-crystalline forms of inorganic compounds is a common motif in biomineralization and has been found in various calcified tissues. The small amount of nonatacamite copper compounds is strongly suggestive of a multipurpose role of copper in the jaw and may hold the key to understanding *Glycera's* exotic choice of material.

Acknowledgment. The authors would like to acknowledge funding by the National Institute of Health under Grant BRP DE014672. H.C.L. was supported by the Fonds zur Förderung der Wissenschaftlichen Forschung under Awards J2184 and T190. H.B. thanks the Danish Natural Sciences Research Council for financial support and the Danish Natural Sciences Research Council and the Danish Technical Research Council for a Steno assistant professor fellowship (21-03-0433) that supported the final stages of the present work. Use of the APS was supported by the Department of Energy (DOE), Office of Science, Office of Basic Energy Sciences, under Contract W-31-109-Eng-38. PNC-CAT facilities at the APS and research at these facilities are supported by the US DOE Office of Science Grant No. DEFG03-97ER45628, the University of Washington, a major facilities access grant from NSERC, and Simon Fraser University.

(25) Waseda, Y. *Anomalous X-ray scattering for materials characterization*, Springer Tracts in Modern Physics; Heidelberg: Springer-Verlag, 2002; Vol. 179.